LA-UR- 98-4850

Title: The Dirac Experiments - Results and Challenges

RECEIVED
AUG 18 1999
OSTI

Author(s): R.G. Clark, J.L. O'Brien, A.S. Dzurak, B.E. Kane, N.E. Lumpkin, D.J. Reilley, R.P.Starrett Natioanl Pulsed Magnet Laboratory and Semiconductor Nanofabrication Facility University of New South Wales, Sydney Australia
D.G. Rickel, MST-NHMFL, J.D. Goettee, LANSCE-9, L.J. Campbell, MST-CMS, C. M. Fowler, DX-3, C. Mielke, MST-NHMFL, N. Harrison, MST-NHMFL, W.D. Zerwekh, DX-7, D. Clark, LANSCE-5, B.D. Bartram, MST-6, J.C. King, DX-4, Parkin, CMS

Submitted to: Physical Phenomena at High Magnetic Fields -III
National High Magnetic Field Laboratory
Tallahassee, Florida- October 24-27, 1998

Los Alamos
NATIONAL LABORATORY

Form No. 836 R5
ST 2629 10/91

DISCLAIMER

The Dirac Experiments - Results and Challenges

R.G. Clark, J.L. O'Brien, A.S. Dzurak, B.E. Kane, N.E. Lumpkin, D.J. Reilley and R.P. Starrett
National Pulsed Magnet Laboratory and Semiconductor Nanofabrication Facility, University of New South Wales, Sydney, Australia

D.G. Rickel, J.D. Goettee, L.J. Campbell, C.M. Fowler, C. Mielke, N. Harrison, W.D. Zerwekh, D. Clark, B.D. Bartram, J.C. King and D. Parkin
Los Alamos National Laboratory, USA

H. Nakagawa and N. Miura
Institute for Solid State Physics, University of Tokyo, Japan

Abstract

The 1997 international Dirac II Series held at Los Alamos National Laboratory involved low temperature electrical transport and optical experiments in magnetic fields exceeding 800T, produced by explosive flux compression using Russian MC-1 generators. An overview of the scientific and technical advances achieved in this Series is given, together with a strategy for future work in this challenging experimental environment. A significant outcome was achieved in transport studies of microfabricated thin-film YBCO structures with the magnetic field in the CuO plane. Using a GHz transmission line technique at an ambient temperature of 1.6 K, an onset of dissipation was observed at 150 T (a new upper bound for superconductivity in any material), with a saturation of resistivity at 240 T. Comparison with the Pauli limit expected at B=155 T in this material suggests that the critical field in this geometry is limited by spin paramagnetism. In preparation for a Dirac III series, a systematic temperature-dependent transport study of YBCO using in-plane magnetic fields of 150 T generated by single-turn coils, at temperatures over the range 10-100 K, has been undertaken in collaboration with the Japanese Megagauss Laboratory. The objective is to map out the phase diagram for this geometry, which is expected to be significantly different than the Werthamer-Helfand-Hohenberg model, due to the presence of paramagnetic limiting. Nanofabricated magnetometers have also been developed in a UNSW-LANL collaboration for use in Dirac III for Fermi surface measurements of YBCO in megagauss fields, which are described.

Introduction

The Dirac Series of experiments was instituted in 1996 at Los Alamos National Laboratory so that a variety of experimental projects could access

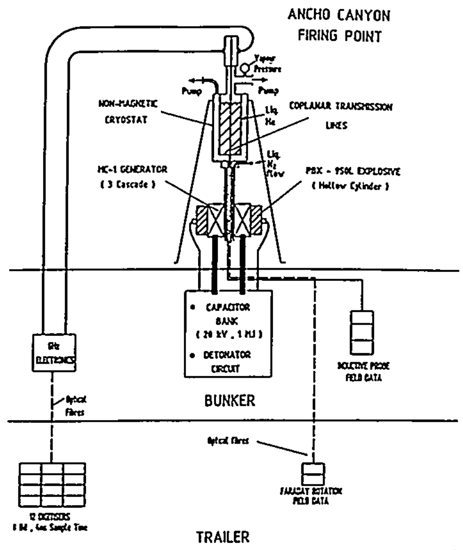

Figure 1. Configuration for implosive flux compression experiments at Los Alamos National Laboratory, USA. The thick lines at top-left represent low-loss cables for the GHz transport measurements.

fields approaching 1000 T for the study of new physical phenomena in condensed matter systems. The second Series was undertaken in 1997 and a third Series is planned for 1999, with the overall program including groups from six nations. Central to this has been a US-Russia collaboration in which Russian-developed MC1-class [1] flux-compression generators have been provided for the experiments. The Series has included studies of magneto-optics in magnetic materials [2] and semiconductors [3], quantum limit effects in organic metals [4] and chemical bond strengths in organic materials [5].

One of the most ambitious experiments within the Dirac Series has been the attempt to obtain reliable transport data on both semiconductor and high-T_c superconductor materials by an Australia-Japan-US team. The experiments required a number of innovations for the elimination of Faraday pick-up [6]. Measurements during Dirac I [6,7] on semiconductor heterostructures demonstrated the success of the technique, paving the way for a fruitful and detailed investigation of the high-T_c superconductor, $YBa_2Cu_3O_{7-\delta}$ (YBCO) during Dirac II. Here we discuss the measurements on YBCO in detail, which have provided the first evidence of paramagnetic limiting in the high-T_c cuprates [8,9], as well as previewing planned experiments for Dirac III in 1999.

Experimental Innovations for μs Transport Measurements

The conditions during an MC1 generator pulse are extreme, with the generator, cryostat and samples all destroyed after the pulse. Fig. 1 shows the experimental arrangement for the low temperature measurements. During the

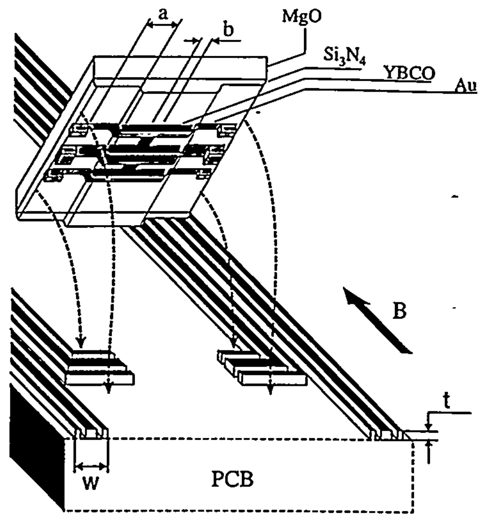

Figure 2. Flip-chip sample mounting. Thin Au transmission lines (80 nm) bridge gaps in the thicker lines on the PCB. Six Au pads (300 nm) provided contacts and the chips were held in place using a heat curable epoxy. Here a=150 μm, b=10 μm, t=9 μm and w=410 μm.

pulse, dB/dt can reach 10^9 T/s, creating voltage up to 1 kV in a conducting loop of area 1 mm^2. Minimization of Faraday pick-up was therefore critical and specially designed [6] coplanar transmission lines (CTLs) patterned on a printed circuit board (PCB) substrate were used to achieve this. Eddy current heating of the CTL connections represented a potential problem, since Cu of thickness 9 μm can heat above 10 K during the field pulse [6]. Thermal isolation of the samples was achieved by patterning thin (80 nm) Au CTLs directly onto the samples, bridging a 2 mm gap in the *thick* CTLs on the PCB (see Fig. 2). To avoid the problem of erratic ohmic contacts at large B, a layer of Si_3N_4 dielectric was sandwiched between the YBCO and the metal CTLs [10], so that the coupling to the sample was capacitive.

Transport Measurements of YBCO to 300 T

We first discuss results obtained during the Dirac-II Series in 1997, which suggest that critical fields in YBCO for $B \perp c$-axis are determined by paramagnetic limiting. The experimental configuration shown in Fig. 2 probes the in-plane resistivity ρ_{ab} of YBCO through its modulation of the transmission S of GHz radiation. If the sample is superconducting the inner and outer conductors of the CTL triplet are shorted so that S is zero, except for a small contribution from cross-talk, whereas a perfect insulator has no effect on transmission. Although the sample impedance at 1 GHz is a complex quantity the measurement provides no phase information so, for simplicity, we assume that the impedance corresponds to a scalar resistivity ρ.

Fig. 3 shows results for T=1.6 K, i.e. $T/T_c \sim 0.02$, in an 850 T MC1 field pulse. Only data to 320 T are plotted, since results above this field were obscured by noise, discussed below. We observe the onset of a dissipative (ρ>0)

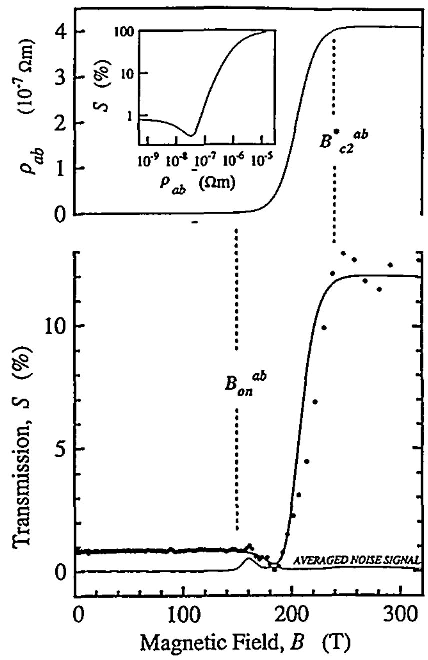

Figure 3. Measured normalised transmission S data (•) for YBCO with $B \perp c$ obtained in an MC1 pulse with T=1.6 K, ν=0.9 GHz and a power ~1 mW at the sample. The bold line is a fit to this S data. A small averaged noise background (fine line) has been subtracted from the data. The upper curve is the calculated resistivity, assuming the transmission function $S(\rho_{ab})$ shown in the inset. The dip in S at $\rho \sim 5 \times 10^{-8}$ Ωm is well understood and results from interference between ingoing and reflected signals on the CTLs. Taken from Ref. [8].

state at $B_{on}{}^{ab}$=(150±20) T and define $B^{*}_{c2}{}^{ab}$=(240±30) T as the field at which S, and therefore ρ, saturates, using an asterix to indicate that the transition may result from paramagnetic limiting. The uncertainties in B reflect the noise-limited accuracy with which we can define inflection points in the S data, together with an estimate of timing accuracy.

To our knowledge $B_{on}{}^{ab}$~150 T is the largest field in which a superconducting phase has been observed. A broader superconductor-normal (S-N) transition than observed here, spanning 75 T - 340 T, has been observed in previous measurements [11,12], possibly due to the high frequency (94 GHz) used. We also note that the strongest saturation feature present in this data [11,12] is near our critical field of 240 T.

To determine the response in Fig. 3 accurately it was necessary to subtract from the raw data a noise background (as shown). Below 300 T the noise is small and occurred in the interval 150 T - 180 T [8], due to the fusion of metal

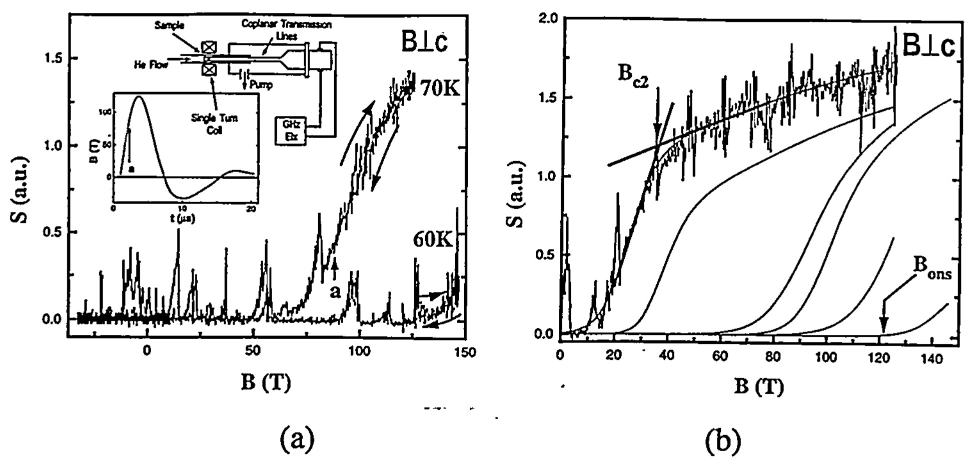

Figure 4. GHz transport data on YBCO obtained in *destructive* single-turn coil pulses to 150 T. (a) Raw transmission S data at T=60 K and 70 K. The inset shows the experimental arrangement and the field profile $B(t)$. Data is shown for times after the arrow marked a in the inset. (b) Magnetoresponse $S(B)$ at T=80 K, 77 K, 70 K, 66 K, 65 K and 60 K, in order of increasing B_{ons}. The curves are fits to the data, with the raw data at 80 K shown for comparison. Also shown are the definitions used for B_{c2} and the onset field, B_{ons}.

wires comprising the second of the three generator liners. Above 300 T wire fusion proceeded in the third liner with the noise creating severe problems for transport measurements. To avoid this problem during Dirac III in 1999, one or two of the inner liners will be removed from the MC-1 generators. Thus configured, the generators are still capable of reaching 400 T, which exceeds the critical field in these samples and offers the opportunity of observing any possible reentrant states above $B^{*}{}_{c2}{}^{ab}$.

Single Turn Coil Measurements of YBCO to 150T

For Dirac II and the coming Dirac III Series, complementary measurements have been made at the Japanese Megagauss Laboratory using single-turn coil pulsed field systems [13] to collect systematic data sets and study dynamic effects through an examination of any hysteresis present. For bore sizes ~10 mm these systems produce ~30 T non-destructively, or ~150 T in pulses which destroy the generator but leave the sample unperturbed. The rise time is ~ 3 μs (see inset to Fig. 4a), giving a peak dB/dt~10^8 T/s which, while around an order of magnitude smaller than the MC1 generators, provides indicative information about dynamic effects.

Results obtained prior to Dirac II using non-destructive pulses to 30 T showed that dynamic effects on a μs timescale are negligible in YBCO with $B \perp c$ [8]. This conclusion has been reinforced in recent measurements using destructive shots to 150 T [14]. Fig. 4 shows GHz transmission S data obtained at a variety of temperatures below T_c. For these measurements it was possible to tune the frequency so that S=0 when the film was superconducting. Transmission increased monotonically with ρ as the sample was driven into the normal state by B. The raw data in Fig. 4 show a number of positive-going perturbations to S corresponding to GHz noise, probably associated with RF emissions from the vaporising coil. The underlying sample response $S(B)$ is clear, however, and has been fitted for a series of temperatures in Fig. 4(b).

As the inset to Fig. 4(a) shows, the coil generates a damped oscillating B which produces a number of cycles before destruction. The raw data in Fig. 4(a) show S over this full period except for the first 2 μs, where large electrical noise obscures the data. Note that there is *no measurable hysteresis* in S between B increasing and decreasing throughout the resistive transition. This is significant, since it implies that the S-N transition is a quasi-equilibrium process, even in μs pulses to 150 T. Dynamic effects associated with flux motion or heating caused by the large dB/dt are clearly not as important as one might suspect, providing confidence in interpretation of the data from Dirac flux-compression measurements.

The critical fields B_{c2} and resistive onsets B_{ons} as defined in Fig. 4(b) are plotted for a detailed data set on a single YBCO sample to create a B-T phase diagram (Fig. 5). B_{c2} varies linearly with T up to ~100 T, with a slope close to the often quoted value dB_{c2}/dT= - 10.5 T/K obtained by Welp *et al.* [15] from magnetisation measurements in magnetic fields up to 6 T.

Discussion and Strategy for Dirac III

It is clear from our data that the low-T S-N transition for YBCO is very different for the two orientations $B \perp c$ and $B // c$. The phase diagram for $B // c$ (inset to Fig. 5a), from Ref. [16], is in good agreement with the BCS model of Werthamer-Helfand-Hohenberg (WHH) which, neglecting contributions from the Zeeman energy of the electron spins, gives $B^0_{c2}(T{=}0) = 0.70\, T_c \left(\partial B_{c2}/\partial T\right)\big|_{T_c}$ [17]. Inserting the slope α=-2.0 T/K gives $B^0_{c2}(T{=}0)$ = 120 T which is consistent with that observed experimentally. Using the same model for $B \perp c$, however, predicts $B^0_{c2}(T{=}0)$ = 625 T which is almost a factor of three greater than the measured value (see Fig. 5b). One explanation is that a misalignment of B could probe properties in the ***a-b*** planes, which would reduce the observed B_{c2}. This effect can be dramatic for highly anisotropic materials such as organic superconductors [18] but should be small for YBCO which has much smaller anisotropy. A more probable explanation is that for $B \perp c$ the Zeeman energy associated with maintaining the singlet state exceeds the superconductor energy gap well before B^0_{c2} is reached. The field B_p at which this occurs is referred to as the paramagnetic (or Clogston) limit which, from BCS theory, is given by $B_p = \gamma T_c$ with γ=1.84 T/K [19]. For our samples we have B_p~155 T, which is above B^0_{c2} for $B // c$ but well below it for $B \perp c$.

Our data may therefore represent the first observation of paramagnetic limiting for a cuprate superconductor, providing additional experimental

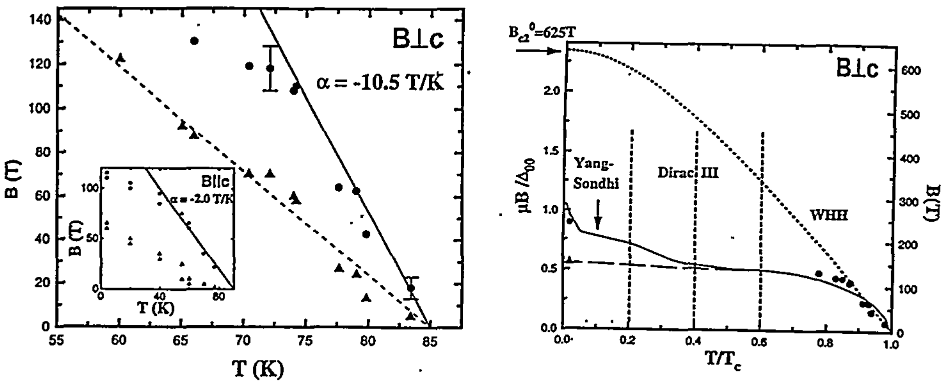

(a) (b)

Figure 5. (a) YBCO phase diagram for $B \perp c$ determined from GHz measurements using single-turn coils. The symbols marked ● (▲) represent B_{c2} (B_{ons}) values as defined in Fig. 4(b). The dashed line corresponds to $dB_{c2}/dT = -10.5$ T/K, determined from magnetisation measurements by Welp et al. [15]. Inset: Phase diagram for $B // c$ determined from transport measurements using single-turn coils [taken from Ref. 16]. (b) Full YBCO phase diagram for $B \perp c$. The symbols ● (▲) represent B_{c2} (B_{ons}) values obtained from MC-1 and single-turn coil data in Figs. 3 and 4. The solid line represents B_{c2} calculated for a $d_{x^2-y^2}$ superconductor while the dashed line depicts a first order transition from a BCS state to a Fulde-Ferrell state [taken from Ref. 20]. The dotted function is the WHH prediction assuming no spin paramagnetism. The vertical lines show planned temperatures for MC-1 shots during Dirac III.

information of relevance to current models of high-T_c superconductivity. Recent interpretations in terms of a $d_{x^2-y^2}$ state have motivated a number of new models. The phase diagram predicted by one model [20], which considers the coupling of B only to the spins of the electrons, is plotted in Fig. 5(b). The agreement with our low-T data is remarkably good. In this model a first order phase transition (dashed line) occurs for $T/T_c < 0.5$ between a zero momentum pairing state at low B and a finite momentum, or Fulde-Ferrel (FF), state at higher B. We note that our low-T B_{ons} coincides with this transition, although ρ would be expected to remain at zero throughout the FF phase. Our data provide a useful preliminary picture of the YBCO phase diagram with strong paramagnetic effects and the primary aim for Dirac III is to complete this diagram, with shots at several temperatures as shown in Fig. 5(b).

Development of de Haas-van Alphen Coils for Dirac III

For the 1999 Dirac III series it is also planned to extend a previous measurement of the de Haas-van Alphen (dHvA) effect and Fermi surface of

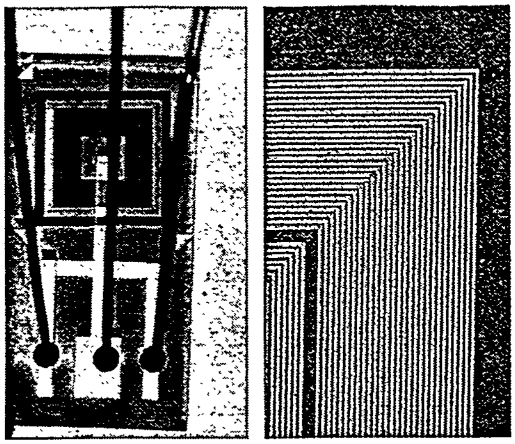

(a) (b)

Figure 6. dHvA coil magnetometers for use in pulsed fields and fabricated at UNSW. (a) Optical micrograph showing full device with bond wires attached. The outermost coil is 450 μm on a side. (b) SEM image showing the individual windings of the coil, fabricated by electron-beam lithography. This coil has 250 nm metal wires with a 250 nm spacing.

YBCO in a 100 T flux compression system [21] to higher magnetic fields. To achieve this aim, it is necessary to develop sensitive, perfectly compensated dHvA coils using electron beam lithography, for use with small samples, which can be connected to the coplanar transmission line geometry that minimises dB/dt pickup in the MC-1 generator environment.

As a first step in this direction, dHvA coils of this design have been fabricated for tests in ms pulsed fields (see Fig. 6). The coil geometry and data taken for a LaB_6 single crystal test sample in a 50 T pulse at 4 K are shown in Fig. 7. For the orientation of this crystal, the three branches of the α frequency

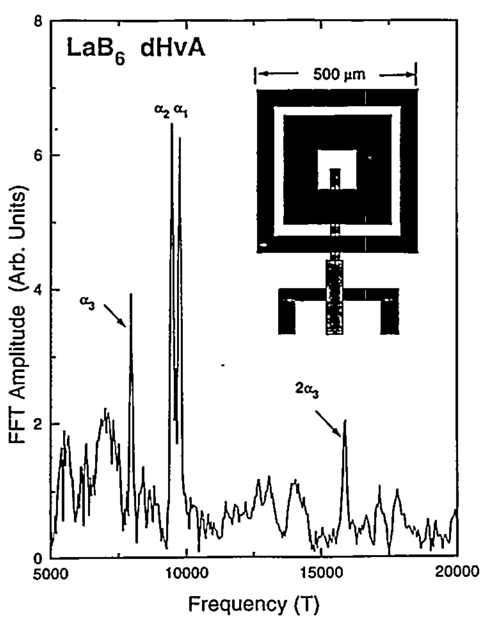

Figure 7. Fourier transform of the dHvA signal measured in LaB_6 at 4 K on the falling magnetic field, analysed over the range 30-50 T in a ms pulse. The single crystal sample with linear dimensions ~200 μm was orientated with the [001] axis at an angle of ~15° to the pulsed field (towards [101]). The inset shows the nanofabricated dHvA coil geometry. Compensated coils with both 0.5 μm and 0.25 μm wide gold lines on a GaAs substrate have been developed, comprised of 46 (181) inner turns and 16 (60) counterwound outer turns, respectively. The coils are designed for connection to coplanar transmission lines developed for the Dirac Series transport measurements.

(α_1, α_2, α_3) [22,23] are clearly observed at 4 K (together with the second harmonic $2\alpha_3$) on a small sample with a coil comprised of only 46 inner and 16 outer windings of 0.5 μm width and 1.5 μm spacing, using a preamplifier gain of only 5000.

A number of technical difficulties remain to be solved for the more stringent environment of the MC-1 shots, associated with details of the connection of the magnetometer coil to the CTLs and screening of the CTLs for dHvA measurements. The ms pulsed field test results are nevertheless encouraging and highlight the importance of nanofabrication technology to advances in megagauss magnetic field measurements.

Conclusions

The Dirac Series has motivated significant innovations for electrical transport measurements in megagauss magnetic fields, allowing a detailed study of the phase diagram of $YBa_2Cu_3O_{7-\delta}$. Our data suggests that with B directed along the CuO planes, paramagnetic limiting determines the upper critical field, the first evidence of this effect in an optimally-doped high-T_c material. Additional developments in nanofabricated dHvA coils provide an opportunity to study the Fermi surface of this important cuprate superconductor above 100 T.

References

[1] A.I. Pavlovskii *et al.*, in P.J. Turchi (Ed.), *Megagauss Physics and Technology*, Plenum, New York, 1980, p. 627.

[2] O.M. Tatsenko *et al.*, *Physica B* **246-247**, 315 (1998); and these proceedings.

[3] J.S. Brooks *et al.*, *Physica B* **246-247**, 50 (1998); and these proceedings.

[4] J.S. Brooks et al., Los Alamos Preprint Report LA-UR 96-3472; J.S. Brooks *et al.*, *Proc. Megagauss VII, Sarov - Russia, 1996.*

[5] A.S. Maverick and L.G. Butler, *Int. J. Quant. Chem.* **64**, 607 (1997).

[6] B.E. Kane *et al.*, *Rev. Sci. Instr.* **68**, 3843 (1997).

[7] B.E. Kane *et al.*, *Proc. Megagauss VII, Sarov - Russia, 1996.*

[8] A.S. Dzurak *et al.*, *Phys. Rev. B* **57**, R14084 (1998).

[9] A.S. Dzurak *et al.*, *Physica B* **246-247**, 40 (1998).

[10] For fabrication details see: N.E. Lumpkin *et al.*, *Physica B* **246-247**, 395 (1998).

[11] J.D. Goettee *et al.*, *Physica C* **235-240**, 2090 (1994).

[12] A.I. Bykov *et al.*, *Physica B* **211**, 248 (1995).

[13] K. Nakao *et al.*, *J. Phys. E* **18**, 1018 (1985).

[14] J.L. O'Brien *et al.*, to be published.

[15] U. Welp *et al.*, *Phys. Rev. Lett.* **62**, 1908 (1989).

[16] H. Nakagawa *et al.*, *Physica B* **246-247**, 429 (1998).

[17] N.R. Werthamer, E. Helfand and P.C. Hohenberg, *Phys. Rev.* **147**, 295 (1966).

[18] S. Wanka *et al.*, *Phys. Rev. B* **53**, 9301 (1996).

[19] A.M. Clogston, *Phys. Rev. Lett.* **9**, 266 (1962).

[20] Kun Yang and S.L. Sondhi, cond-mat/9706148 v2 (1998).

[21] C.M. Fowler *et al.*, *Phys. Rev. Lett.* **68**, 534 (1992); and Comment by M. Springford, P. Meeson and P-A. Probst, *Phys. Rev. Lett.* **69**, 2453 (1992).

[22] Y. Ishizawa *et al.*, *J. Phys. Soc. Jap.* **42**, 112 (1997).

[23] N. Harrison *et al.*, *Phys. Rev. Lett.* **80**, 4498 (1998).